

Daniel Diffendale ORCID iD: 0000-0002-5508-9458

Combining geochemistry and petrography to provenance Lionato and Lapis Albanus tuffs used in Roman temples at Sant’Omobono, Rome, Italy

Daniel P. Diffendale¹, Fabrizio Marra², Mario Gaeta³, Nicola Terrenato¹

¹ Department of Classical Studies, University of Michigan, 2160 Angell Hall, 435 S. State St., Ann Arbor, MI, 48109-1003, USA.

² Istituto Nazionale di Geofisica e Vulcanologia, Rome, Italy

³ Dipartimento di Scienze della Terra, Sapienza-Università di Roma, Italy

corresponding author: Daniel P. Diffendale

diffenda@umich.edu

ABSTRACT

Tufo Lionato is a volcanic tuff that was used extensively for construction in Rome, Italy, during antiquity and after; at least three varieties can be identified: Anio, Monteverde, and Portuense. The widespread introduction of Tufo Lionato in Roman construction is generally dated to the mid-2nd century BCE. Another tuff, Lapis Albanus, is held to have been introduced during the 3rd century BCE. Due to their similar macroscopic appearance, it is impossible to reliably distinguish visually among varieties of Tufo Lionato, or between Lapis Albanus and other ‘peperino’ tuffs, nor does geochemistry alone always allow definitive identifications. A combination of geochemical and petrographical analyses is presented here, in order to provenance building stone from the Roman temples of Fortuna and Mater Matuta at Sant’Omobono in Rome. The combination of techniques allows for secure identification of Anio tuff and Lapis Albanus, and their use in structures of the 4th–3rd and 5th–3rd centuries BCE, respectively, one to two centuries earlier than previously demonstrated. These findings show a diversification of tuffs used by the Roman construction industry earlier than

This is the author manuscript accepted for publication and undergone full peer review but has not been through the copyediting, typesetting, pagination and proofreading process, which may lead to differences between this version and the [Version of Record](#). Please cite this article as [doi: 10.1002/gea.21702](https://doi.org/10.1002/gea.21702).

This article is protected by copyright. All rights reserved.

henceforth acknowledged, and suggest the ability of archaeometric techniques to bring new perspectives even to such familiar archaeological contexts as the city of Rome.

Keywords: Ancient Rome; Building stones; Volcanic rocks; Trace-element analysis; Petrographic analysis

1 INTRODUCTION

The numerous volcanic stones (“tuffs”, Italian *tufi*) of the Lazio region of central Italy were exploited as building material in the city of Rome beginning at least in the 6th c. BCE (Jackson & Marra 2006). For many years archaeologists have attempted in good faith to identify the various varieties of tuff used in ancient Roman construction on the basis of visual examination alone, but recent work on the geochemical composition of those stones has proven the inefficacy and unreliability of visual differentiation (Jackson et al. 2005; Marra et al., 2011; 2015; 2017; Marra & D’Ambrosio, 2013; Farr et al., 2015). Trace element features of the Lazio tuffs, however, provide accurate and reliable identification criteria to discriminate eruptive products and their source areas (e.g., Peccerillo, 2005; Lustrino et al., 2011). In particular, trace elements with a relatively low mobility, such as Zr, Nb, Y, Th, and Ta, can be successfully used to recognize eruptive products and their provenance, even in the deeply altered volcanic rocks employed in ancient Roman architecture (Marra et al., 2011, 2015; Marra & D’Ambrosio, 2013; D’Ambrosio et al., 2015; Farr et al., 2015). The combination of trace-element, petrographic, and other analyses (such as laser ablation inductively coupled plasma mass spectrometry or LA-ICPMS) has begun to be employed in provenance studies elsewhere in the Roman world (e.g., Germinario, Hanchar, et al., 2018; Germinario, Zara, et al., 2018) that have demonstrated the ability of archaeometry to speak effectively to cultural and historical questions.

As a result of these developments, not only the identification of the Roman tuffs, but also their chronology of use needs re-examining. The prevailing chronological scheme for ancient tuff use largely relies on the study of Lugli (1957), itself drawing on the fundamental work of Frank (1924), who linked the initial exploitation of various tuffs with the expansion of Roman political power chronicled by ancient Roman historians such as Livy. In order to refine this chronology and decouple it from the not always reliable historical record, we have sampled and analyzed tuffs used in archaeologically datable monuments at the site of Sant’Omobono (Figures 1, 2, 3). Located at the southern

This article is protected by copyright. All rights reserved.

foot of Rome's Capitoline Hill, the church of Sant'Omobono overlies an archaeological site comprising some three millennia of human activity, stretching from a 12th century BCE floodplain occupation, to a small early 6th c. BCE temple, massive 5th c. BCE twin temples, and a medieval church rebuilt in the 15th c. CE and still in use today (Terrenato et al., 2012; Brock & Terrenato, 2016; Diffendale et al., 2016). Below the 1930s brickwork sheathing the church and the travertine blocks that compose parts of the Roman temple superstructure, the bulk of the architectural stone is tuff. All of the dimension stone used in the ancient temples and their precinct from the 6th through the 1st c. BCE is in one or another variety of tuff. Only in the 1st c. BCE are other stones such as travertine first employed at Sant'Omobono.

The site's first excavator, Colini, identified the large square platform (47 m²) that gives the sanctuary its overall shape as being built in *peperino* tuff around a core of *cappellaccio* tuff and earthen fill, with a pair of *peperino* altars in front of the temples (Colini, 1938). In subsequent work, a pavement of the temples in stone slabs and the pavement in front of the temples in stone blocks have been identified as a mixture of Anio and Monteverde tuff (Torelli, 1968; Coarelli, 1988 speaks only of *grossi blocchi di tufo* ("large blocks of tuff") without further identification; Holloway, 1994 refers only to Monteverde). A pavement in thin slabs of Tufo Lionato, dated to a reconstruction of the sanctuary in 212 BCE, has consistently been described in previous literature as Monteverde tuff (Colini, 1962; Mercado, 1962; Sommella, 1968; Torelli, 1968; Coarelli, 1988; Holloway, 1994). No systematic identification of all of the building stones used at Sant'Omobono has ever been published. In 1970, however, G. Pisani Sartorio prepared a plan of the excavated area in which she identifies the material of each block. Pisani Sartorio distinguishes between seven types of tuff (the modern geological names for which we add in parentheses): Anio (Tufo Lionato - Anio facies), Grotta Oscura (Tufo Giallo della Via Tiberina), Monteverde (Tufo Lionato - Monteverde facies), Fidene (Tufo Rosso a Scorie Nere), *cappellaccio* (usually Tufo del Palatino), *peperino* (often Lapis Albanus), and *pietra gabina* (Lapis Gabinus). In order to clarify the provenance and identification of ashlar building stone employed at Sant'Omobono, multiple features within the archaeological area were sampled for geochemical and petrographic analysis.

2. TUFFS EMPLOYED AS DIMENSION STONE AT SANT'OMOBONO

2.1 Tufo Lionato (Anio, Monteverde, and Portuense Facies)

Until recent work by Marra et al. (2017), which identified a Portuense facies, archaeologists had recognized only two *facies* or varieties of the volcanic rock known by the geological name of Tufo Lionato: Monteverde and Anio (Italian *Aniene*), after the known ancient extraction areas located in Monteverde on the west bank of the Tiber River, and in several localities along the Anio River, respectively (Marra et al., 2017; Jackson & Marra 2006; Quilici 1974). According to the chronological scheme proposed by Lugli (1957), Monteverde tuff was used from the 3rd century BCE, Anio tuff from the mid-2nd century.

Marra et al. (2017) have demonstrated that no objective criterion based on macroscopic visual inspection alone is sufficient to identify the provenance of samples of Tufo Lionato. In contrast, using a new method of classification based on the ratio of immobile elements (e.g., Marra et al., 2011; 2015; Marra & D'Ambrosio, 2013; Farr et al., 2015), these authors have shown that four samples of Tufo Lionato, collected at different locations in Monteverde and the nearby area of Portuense, yielded homogeneous Zr/Y vs Nb/Y composition that distinguished them from five samples collected at quarry sites in the Anio valley and on the Capitoline hill.

Using this geochemical fingerprint to determine the provenance of several samples of building stones from Temples A, B, and C in the so-called Area Sacra di Largo Argentina, Marra et al. (2017) have demonstrated that Tufo Lionato from the Anio valley, rather than Monteverde tuff as reported by Marchetti Longhi (1932) and Lugli (1957), was widely employed in the early construction phase of Temple C, dated to the 3rd century BCE (Coarelli, 1981). They have shown, moreover, that all of the previous identifications of Monteverde tuff in Temples A, B, and C at Largo Argentina reported in the archaeological literature have been incorrect, and that Monteverde tuff was used only occasionally in the substructure of the staircase of Temple C, together with Anio tuff and Tufo Giallo della Via Tiberina. Further, a peculiar lithofacies of Tufo Lionato occurring in the Portuense district, close to Monteverde, was used in at least two slabs of the 2nd century BCE platform in front of Temple C, also mixed with the abovementioned tuffs.

Integrating the analysis of the macroscopic lithologic aspect with petrographic observation of thin sections using an optical microscope, Marra et al. (2017) have shown that the rock facies cropping out in Monteverde is characterized by a fine grain-size ash matrix and by a rarity of lithic clast inclusions and loose crystals, which by contrast are abundant and coarser in size in the rock facies occurring along the Anio valley. Moreover, cm-sized carbonate and lava lithic clasts are commonly detected at the macroscopic scale only in the Anio facies. A third rock facies has been determined to occur only in the southernmost urban outcrops on the western bank of the Tiber River, in and around Via Portuense. This is a very fine ash deposit, lacking any lithic clast inclusion or mineral phase.

By comparing the macro- and microscopic features of the sampled architectural blocks with those of rock samples from Monteverde and the Anio valley, it became apparent that in most instances blocks previously interpreted as originating in Monteverde were characterized by a medium-fine grain size and lack of large lithic clast inclusions. This feature was not always so evident, however, as in the facing of the podium of Temple C at Largo Argentina. In particular, the slabs used in the 3rd century facing of Temple C display sub-cm sized scoriae and abundant pyroxene crystals, and look almost identical to those used in the facing of Temple A (dated to the late 2nd century), which Lugli reported as Anio tuff. As noted by Marra et al. (2017), the criteria upon which archaeologists have based identification of Monteverde tuff are unclear, and probably rely mostly on a simple chronological assumption. Indeed, Frank (1924) simply mentions the "brown tuff variety of Monteverde," while Lugli (1957) warns of the close resemblance between Anio and Monteverde tuffs, without indicating any features for distinguishing between them.

In conclusion, the only objective criterion to determine provenance from the Monteverde exploitation area, as opposed to the Anio, is Zr/Y vs Nb/Y composition. Marra et al. (2017) have explained the different geochemical signature as due to the different eruption phases of the Alban Hills volcano that emplaced the deposits in Monteverde, the Anio valley, and central Rome. In particular, those at Monteverde and Portuense are interpreted as the earliest surge deposits, characterized by a petrologically more differentiated magma, compared to the later, scoria-and-block deposits, enriched with lithic clast inclusions, that were emplaced in the Anio valley. This discrimination

method, however, is subject to uncertainties, possibly linked to the variability of the geochemical composition of each eruptive unit—which in turn may be due both to the degree of evolution of the magma during eruption and to the proportion of lithic clast inclusions—as well as to analytical errors during laboratory procedures. Therefore, results should be handled with care, and the integration of different discrimination diagrams (e.g.: Th/Ta vs Nb/Zr; Zr/TiO₂ vs Nb/TiO₂), as well as with other petrographic (i.e., observation in thin section using an optical microscope) and geochemical (i.e., EMP glass analyses) data, whenever applicable, is necessary.

2.2 Lapis Albanus

The name "*peperino*" has been used to indicate a variety of different volcanic rocks used in ancient Roman architecture, all characterized by a similar macroscopic aspect (Farr et al., 2015, for a review). The most common comes from the ancient quarries located at Marino in the Alban Hills southeast of Rome, identified with the ancient *Lapis Albanus* and known by the geological name of "*Peperino albano*" (Freda et al., 2006; Farr et al., 2015). Lapis Albanus is a pyroclastic flow deposit characterized by a lithified, granular texture and gray color, with a typical "*peperino*" (peppercorn) aspect provided by white and black lithic inclusions: carbonate fragments; holocrystalline rocks; abundant, poorly-vesicular scoriae; leucite; and pyroxene crystals. According to Lugli (1957) this rock began to be employed in Roman dimension stone architecture during the 3rd c. BCE (in the Carcer Tullianum; see also Karner et al., 2001), although the results of recent geochemical analysis from Sant'Omobono suggest that this date should be moved back to the early 5th c. BCE (Farr et al., 2015; Diffendale et al., 2016). Another "*peperino*" rock widely used in Rome since at least the 2nd c. BCE is *Lapis Gabinus*, a hydromagmatic eruptive product of the Castiglione Crater (Farr et al., 2015). A third volcanic rock for which the name "*peperino*" has been occasionally used is Tufo del Palatino, whose typical facies, characterized by poor compressive strength and a laminar aspect ("*cappellaccio*"), was employed in Roman construction beginning in the archaic period. Finally, the name "*peperino*" is commonly used for several very hard volcanic rocks of the Vulsini district ("*Peperini listati*," "*Piperno*").

Farr et al. (2015) have shown that the three "*peperino*" stones from Rome, including a particularly coherent rock facies of Tufo del Palatino, known by the local name of "*Peperino della Via Flaminia*," can be readily distinguished by the combined

use of the Zr/Y vs. Nb/Y, Zr/TiO₂ vs. Nb/TiO₂, and Th/Ta vs. Nb/Zr discrimination diagrams. The latter diagram in particular offers a means of identifying Lapis Albanus, through its distinctively low (<35) Th/Ta ratio.

3 SAMPLING AND METHODS

A total of thirty-two samples of tuff were collected from archaeological structures at Sant'Omobono. Twenty-two samples (GS 1, 5–12, 14, 16–21, 24–28, 31) of Tufo Lionato blocks employed in several structures spanning the 4th/early 3rd century through the late 3rd century BCE, and attributed in the literature to both the Anio and the Monteverde facies (Sommella, 1968; Torelli, 1968; Pisani Sartorio, 1970), were collected and analyzed for trace-element composition (Figure 3 and Table 1). Notably, even blocks from the same structures were reported as Anio and Monteverde tuff, independent of their age of employment. Seven samples (GS 2, 3, 4, 13, 15, 29, 30) pertaining to different structures spanning the 5th through 3rd centuries BCE, visually identified or reported as "*peperino*" by Pisani Sartorio, were collected and analyzed for trace-element composition. Three further visually-identified "*peperino*" samples include two samples collected from an inscription dedicated by M. Fulvius Flaccus in 264 BCE (GS 22, 32) and one sample collected from a post-antique stair tread (GS 23).

In this paper we combine petrographic observation in thin section with trace-element analyses of the investigated rocks. Bulk samples of the volcanic rocks and the building stones were analyzed for major and trace element composition at Activation Laboratories, Canada by Lithium Metaborate/Tetraborate Fusion ICP-MS. The fused samples were diluted and analyzed by Perkin Elmer Sciex ELAN 6000, 6100 or 9000 ICP/MS. Three blanks and five controls (three before the sample group and two after) were analyzed for each group of samples. Wet chemical techniques were used to measure the loss on ignition (LOI) at 900°C. International rock standards have been used for calibration and the precision is better than 5% for Rb and Sr, 10% for Ni, Zr, Nb, Ba, Ce, and La, and 15% for the other elements. Full geochemical data are provided as supplementary online material (Appendix 1).

4 RESULTS

4.1 Tufo Lionato

4.1.1 *Macroscopic Features*

Pisani Sartorio seems to have used overall grain size to distinguish between the Anio and Monteverde facies. On careful examination, however, only GS 5, 9, and 21, among those attributed to Monteverde (GS 5, 7, 9, 10, 16, 21, 24, 25), are characterized by very fine grain size and lack of lithic clast inclusions, displaying a "sandy" texture similar to that of the Tufo Lionato facies cropping out in Monteverde (see GS 21a and MV-A in Figure 4). When examined in greater detail, these samples revealed other macroscopic features contrasting with those typical of the Monteverde facies. Once split, GS 21 revealed the presence of two large (ca. 1 cm) orange scoriae (GS 21b in Figure 4), and one leucite crystal ca. 0.5 cm in diameter, which constitute a quite uncommon occurrence (especially concentrated in such a small fragment) in the Monteverde facies. The other two fine-grained samples (GS 5, 9) display abundant, yet very small leucite crystals.

More generally, photos of representative samples of supposed Monteverde and Anio facies in Figure 4 show a gradual variation in grain size and lithic clast/mineral occurrence, from those characterized by the typical Anio facies (GS 1, 8) with abundant leucite and pyroxene crystals, grey scoriae, and lava and carbonate lithic clasts, passing through those displaying intermediate features (GS 6, 14, 16), to those (GS 7, 21) displaying a texture most similar to that of the Monteverde facies (MV-A).

In particular, it is not possible to objectively distinguish between GS 6 (previously reported as Anio) and GS 21b (previously reported as Monteverde) at the macroscopic level. Similarly, there is no reason to consider GS 16—which, despite its fine-grained matrix, is characterized by the presence of abundant leucite crystals, grey scoriae and carbonate lithic clasts—as Monteverde rather than Anio facies. Indeed, samples GS 6, 7, 14, and 16 display medium-coarse grain size and "sandy" texture, compatible with the Monteverde facies, but were attributed both to Anio (GS 6, 14) and to Monteverde (GS 7, 16). Such a medium-coarse, sandy texture was also observed in several blocks of the 2nd century platform in front of Temple A at Largo Argentina,

attributed to the Monteverde facies by Lugli (1957), but recently recognized as the typical Anio facies based on trace-element composition (Marra et al., 2017).

4.1.2 Microscopic Features

Four samples of Tufo Lionato blocks were chosen for analysis in thin section using an optical microscope. These samples were selected because, while they all had geochemical signatures similar to those of the Monteverde facies, two were attributed by Pisani Sartorio to the Anio facies (GS 6, 14) and two to Monteverde (GS 16, 21). Their petrographic features are compared with those characteristic of the Portuense, Monteverde, and Anio facies described in Marra et al. (2017), and here summarized in Table 2.

Sample GS 21

This sample displays matrix-supported texture with both calcite and zeolite in the matrix, fine to coarse ash grain size with poor sorting, porphyritic juvenile with orange glass including clinopyroxene phenocrysts; moderately thick mica crystals are present. All of these features are characteristic of the Anio facies, allowing us to rule out a provenance from the Monteverde rock-type.

Sample GS 16

Matrix-supported, poorly sorted, with lapilli-sized scoriae and tuff lithic clasts, porphyritic juvenile with clinopyroxene and mica phenocrysts; mm-sized leucite crystals are altered into calcite and zeolite (Figure 5). These features indicate a typical Anio facies.

Samples GS 6 and GS 14

These samples are matrix-supported and very poorly sorted, with abundant limestone and lava lithic clasts, and scoriae up to 1 cm in diameter. Abundant leucite turned into calcite and zeolite, clinopyroxene and thick mica crystals are present. These features indicate the typical coarse Anio facies as observed at the Salone quarries in the Anio River valley (Marra et al., 2017).

In conclusion, the petrographic and textural features of samples GS 6, 14, 16, and 21 allow us to rule out a provenance from Monteverde, despite macroscopic features (fine grain size and paucity of lithic clast inclusions, in, e.g., GS 6, 21), trace-element composition (e.g., GS 16, 21, see next section), or previous attribution (GS 14, 21), that suggested their possible origin in that quarry area.

4.1.3 Trace-element discrimination diagrams

Zr/Y vs Nb/Y compositions of the samples analyzed in this work are shown in the discrimination diagram of Figure 6. The composition of outcrop samples of the different Tufo Lionato lithofacies determined by Marra et al. (2017) is reported in the diagram of Figure 6, along with compositional fields for Tufo Lionato (TL), Tufo del Palatino (TP), Lapis Albanus (LA) and Lapis Gabinus (LG) previously determined on the basis of samples analyzed by Farr et al. (2015). An overall correspondence in the distribution of SO samples previously reported as Anio/Monteverde facies with respect to the literature compositional field of Tufo Lionato is observed in Figure 6.

The newly analyzed samples, however, also exhibit an overall upward translation with respect to the corresponding fields identified in Farr et al. (2015). This is likely the effect of a laboratory trade-off that can affect batches of samples analyzed in different runs, as remarked upon by Marra et al. (2015); the analytical precision of the measurement can be on the order of up to 15% for Y and 10% for Zr and Nb. This limitation, then, should be taken into account when discussing the attribution of the analyzed samples to the Monteverde or Anio facies. If regarded based on the compositional boundary determined in Marra et al., 2017 (solid red line separating the Anio (AN) from the Monteverde (MV) compositional field), none of the previous attributions to the Monteverde facies is confirmed for the analyzed blocks, with the exception of the very anomalous composition of GS 25. Indeed, all the other samples collected from blocks attributed to this facies plot above the compositional boundary, within the Anio field. When a possible laboratory discrepancy is considered and assessed using as upper boundary for the Monteverde field (dashed red line) the composition of two control samples of the Anio facies (X-1, X-2) analyzed with those collected at SO, four samples plot within the enlarged Monteverde compositional field (yellow area).

Notably, the two uppermost samples (GS 8, 14) were previously identified as Anio tuff, and their macroscopic and microscopic texture (see Figure 4 and previous section) confirm this attribution, consistent with Marra et al.'s definition of the compositional boundary. GS 16, moreover, also displays a high frequency of lithic and mineral inclusions, a lack of granulometric sorting, and other petrographic features that provide an unequivocal attribution to the Anio facies. Only GS 21, then, could be possibly regarded as Monteverde facies, given its geochemical fingerprint very close to the compositional boundary in the discrimination diagrams of Figure 6 and 7, and its fine grain size with absence of lithic inclusions. The occurrence of large orange scoriae and leucite crystals (Figure 4), however, coupled with its microscopic character, are petrographic features typical of the Anio facies.

Sample GS 25 plots as an outlier also in the Th/Ta vs Nb/Zr diagram (Figure 7), far beyond the compositional boundary of the Anio facies. This sample, however, is affected by a very anomalous Zr content, much lower than the average of all the other samples analyzed thus far. We have checked its geochemical fingerprint with an alternative diagram, based on Th/Ta vs Nb/Y, in order to overcome the Zr anomaly (Figure 8). In this case, sample GS 25 plots well inside the overall Tufo Lionato compositional field but far from the Monteverde outcrop samples and from the two archaeological samples with similar composition (GS 16 and 21), while it is one of the most offset within the Anio field, suggesting attribution to this latter facies. In sum, none of the analyzed samples—including those displaying macroscopic aspects most similar to the Monteverde facies (GS 16, 21)—can be regarded as originating in the Monteverde quarry area.

4.2 Peperino Albano and Tufo del Palatino

4.2.1 *Macroscopic Features*

Although the macroscopic aspect of all visually-identified peperino samples was consistent with an identification as Lapis Albanus, the early date attributed to the sampled structures, preceding the earliest attested employment of this rock so far, in the Carcer Tullianum—suggested to date to the 3rd century BCE (Lugli, 1957; Karner et al., 2001)—requires a careful assessment of their provenance. Accordingly, we have analyzed these samples for their trace-element composition, to compare with those of

Lapis Albanus and of the typical "*cappellaccio*" and "*Peperino della Via Flaminia*" facies of Tufo del Palatino, previously analyzed by Farr et al. (2015).

4.2.2 Trace-element Discrimination Diagrams

The discrimination diagrams of Figure 7 and 8 are less effective than the Zr/Y vs Nb/Y diagram in discriminating the Anio and Monteverde facies (see also Marra et al., 2017), as evidenced by the overlapping compositions of a few samples. In contrast, the two diagrams of Figure 7 and 8 provide a straightforward identification for the Lapis Albanus samples, which in the Zr/Y vs Nb/Y diagram partially overlap with that of Lapis Gabinus. The Th/Ta of these samples is lower than that of all other samples and plots within the Albano compositional field defined in previous work (Marra & D'Ambrosio, 2013; Farr et al., 2015), allowing us to attribute to Lapis Albanus all the samples previously reported as *peperino*, as well as the three other samples from SO (GS 22, 23, 32).

5 DISCUSSION

None of the analyzed samples—including those displaying macroscopic aspects most similar to the Monteverde facies (GS 16, 21)—can be regarded as originating in the Monteverde quarry area. The positive identification of Anio tuff confirms the early use of this facies in Roman urban construction already suggested by analysis of samples from Temple C at Largo Argentina, dated as early as the late 4th or early 3rd century (Marra et al., 2017). In contrast, however, to the evidence from Largo Argentina, where the occasional employment of Monteverde tuff in structures otherwise composed of Anio tuff was observed, combined trace-element composition and thin-section petrographic analyses rule out any occurrence of Monteverde in the 4th-3rd century pavements at Sant'Omobono. Indeed, while the contextual occurrence of the idiosyncratic Portuense facies at Largo Argentina proved the mixed provenance, the lack of this facies among the blocks employed at Sant'Omobono may be regarded as further supporting evidence of their homogeneous provenance from the quarries located along the Anio River.

Our analyses provide further confirmation for the use of Lapis Albanus in the facing of the first-phase (5th century BCE) platform supporting the twin temples of Fortuna and Mater Matuta (Diffendale et al., 2016). This had already been suggested by the results of Farr et al. (2015), who sampled a single block (SO-2) forming part of the

eastern edge of the platform at its southern end. The present study adds two samples of the same structure, from midway along the eastern edge of the platform (GS 30) and its northern edge behind Temple A (GS 3), both identified here as Lapis Albanus (see Figures 6, 7, 8). Lapis Albanus (GS 29) was also identified in part of the exterior of the platform of the temples in the reconstruction after 213 BCE.

The use of Lapis Albanus was confirmed for several monuments within the temple platform, which had previously been identified more generally as “*peperino*” (Diffendale, 2016). These include the square cippus within the cella of Temple A (GS 2), the lining of a votive pit within the northern stylobate of Temple A (GS 4), the eastern Republican altar (GS 15), the upper molding of the circular monument (GS 13), and two blocks (GS 22 and 32) of the Fulvius inscriptions dated to 264 BCE (Torelli, 1968; Diffendale, 2016). Finally, Lapis Albanus was used for a block identified as a post-antique stair tread (GS 23), which might have belonged to one of the buildings demolished during clearance of the site in 1936 (Terrenato et al., 2012).

According to Holloway (1994), the Fulvius inscriptions of 264 BCE are the earliest dated use of Lapis Albanus at Rome. They remain the earliest use datable epigraphically, but the use of Lapis Albanus in the platform of the first phase of the twin temples predates these inscriptions by some two centuries. The altar is associated with a pavement that may date to the 4th century BCE, while the cippus is of uncertain date but could date to the late 4th or early 3rd centuries. The platform exterior and the individual monuments thus push back the use of Lapis Albanus at Rome some two centuries earlier than previously acknowledged. The stair tread attests to the continuing use of Lapis Albanus at Rome after the end of antiquity.

The results of the analyses on Tufo Lionato provide further evidence of the inadequacy of visual criteria alone in discriminating between the various facies. The wide use of Monteverde tuff at Sant’Omobono reported in previous publications is not supported by the present study. We have pointed out that previously the sole criterion for identification of the Monteverde facies seems to have been visual observation of a finer grain-size. Our macroscopic and microscopic observations, however, combined with trace-element analysis, have shown that all the blocks displaying a macroscopic aspect similar to that which characterizes the Tufo Lionato cropping out in Monteverde in fact

have the distinctive petrographic and geochemical features of tuff from the Anio quarries.

GS 21, in particular, which, among those blocks previously identified as Monteverde, is the one characterized by a macroscopic aspect and trace-element composition most similar to those pertaining to this rock facies, is part of the Lionato block pavement, from which derive GS 9, 25, 26, and 27, all displaying typical Anio tuff features (Figure 6). The other Monteverde-like sample (GS 16) is a block that supports the Lapis Albanus base molding of the eastern altar; the block on which it rests (GS 14) is part of the same foundation, but was previously attributed to the Anio facies, an attribution readily confirmed by our trace-element and petrographic analyses (Figure 6 and Table 2).

A pavement of the twin temples in slabs of Tufo Lionato, dated to the late 4th or early 3rd century BCE, uniformly employed the Anio facies (GS 1, 5, 6), as did a low staircase associated with this slab pavement (GS 7, 8, 10, 12, 24) and a drain beneath the staircase (GS 11). Very similar slabs were used in the plateaus of the two altars, and one of these also returned results indicative of Anio tuff (GS 17).

The reconstruction of the twin temples following a fire in 213 BCE employed Anio tuff for its pavement (GS 20) as well as in parts of the perimeter wall (GS 28 and 31). The upper course of this platform perimeter was built using Lapis Albanus (GS 29), while the foundations of this phase that were not exposed to the elements were built using macroscopically identified Tufo Giallo, presumably Tufo Giallo della Via Tiberina. Though the latter blocks at Sant'Omobono have not been subjected to geochemical analysis, no other varieties of Tufo Giallo are known in Roman construction (Marra et al., 2011); such analysis is, however, a desideratum for future research. The Lapis Albanus votive pit (GS 4) may belong to this phase. Finally, two architectural elements of general Mid Republican date (4th to 2nd century BCE) have signatures consistent with Anio tuff (GS 18 and 19). GS 18 is a column drum, while Sample 19 is a column base or capital.

The results of these analyses on Tufo Lionato elements from Sant'Omobono thus demonstrate the extensive use of Anio tuff earlier than the mid-2nd century BCE date posited by Lugli and others. Its earliest securely attested use in the Republican precinct is

in the block pavement in front of the twin temples, at some point within the 4th century BCE. Not long after, in the late 4th or early 3rd century, possibly as late as 264 BCE, the temples were rebuilt and paved with exclusively Anio tuff. Anio tuff was also used extensively in the post-213 BCE reconstruction of the temples. A 4th century date is significant, as it attests a growing catchment area supplying the Roman construction industry, and these findings place the initial Roman exploitation of Anio tuff in a similar period as that of Tufo Giallo della Via Tiberina and Tufo Rosso a Scorie Nere.

No Monteverde or Portuense tuff has so far been identified in any structure of any period at Sant'Omobono. This is perhaps a counterintuitive finding, since the Monteverde and Portuense quarries lie much closer to Sant'Omobono than do the Anio quarries. This may have to do with ease of transport, however, as the former quarries are downstream from Sant'Omobono, while the latter lie upstream. The clustering of Anio quarries along the eponymous river had already suggested the importance of waterborne transport (Quilici 1974) and, while today the Tiber flows some 120 m west of Sant'Omobono, in the 4th and 3rd centuries the river lay much closer to the site (Brock 2017, with further references), which would have facilitated riverine supply of building stone.

The Lapis Albanus quarries, on the other hand, lie far from any river system, and their products must have been transported overland, either 20 km northwest directly to Rome, or 17 km north to the Anio and thence by watercraft. Evidently the superior durability of the stone and its ability to take carved detail were sufficiently desirable to justify the cost of overland transport, at least for some applications; indeed, at Sant'Omobono the use of Lapis Albanus seems to have been restricted to the uppermost courses of the temple podium and to specialized features such as altars and other monuments.

6 CONCLUSIONS

The results here presented demonstrate that macroscopic analysis alone is insufficient to distinguish between varieties of Tufo Lionato used in ancient Roman construction. They confirm that a combination of microscopic (petrographic thin-section) and geochemical analyses is required to securely identify samples of Tufo Lionato as belonging to the Anio, Monteverde, or Portuense facies. Further, Anio tuff was

introduced into Roman construction by the early 3rd century BCE, if not already in the 4th century, at least a century earlier than previously demonstrated. Contrary to previous scholarship, no Monteverde tuff has been identified in construction of any period at Sant'Omobono. All of the macroscopically-identified *peperino* stone used at Sant'Omobono is geochemically identified as Lapis Albanus. The results presented here suggest the need for a much wider campaign of sampling and analysis of the Roman tuffs, given the unreliability of previous studies.

ACKNOWLEDGMENTS

The Sant'Omobono Project is promoted by the Sovrintendenza Capitolina ai Beni Culturali in collaboration with the Università della Calabria and the University of Michigan. This work would not have been possible without the support and collaboration of the Sovrintendenza Capitolina ai Beni Culturali, Claudio Parisi Presicce, and Monica Ceci. We acknowledge the constructive comments of the anonymous reviewers for *Geoarchaeology*. Special thanks to Jason Farr for crucial assistance in the earlier stages of this research. This research received funding from the Etruscan Foundation and the University of Michigan College of Literature, Science, and the Arts. This article is based upon work supported by the National Science Foundation under Grant No. 1259122; any opinions, findings, and conclusions or recommendations expressed in this material are those of the authors and do not necessarily reflect the views of the National Science Foundation.

REFERENCES

- Blake, M. E. (1947). *Ancient Roman construction in Italy from the prehistoric period to Augustus*. Washington, D.C.: Carnegie Institution.
- Brock, A. L., & Terrenato, N. (2016). Rome in the Bronze Age: late second-millennium BC radiocarbon dates from the Forum Boarium. *Antiquity*, **90**, 654–664. doi:10.15184/aqy.2016.65
- Brock, A. L. (2017). Floodplain occupation and landscape modification in early Rome. *Quaternary International*, **460**, 167–174. doi:10.1016/j.quaint.2016.05.026
- Colini, A. M. (1938). Zona dei Fori Olitorio e Boario. *Bullettino della Commissione Archeologica Comunale di Roma*, **66**, 279–282.
- Colini, A. M. (1962). Introduzione allo studio dell'area sacra di S. Omobono. *Bullettino della Commissione Archeologica Comunale di Roma*, **72**, 3–6.

Coarelli, F. (1981). Topografia e Storia. In I. Kajanto, U. Nyberg, & M. Steinby (Eds.), *L'area sacra di Largo Argentina* (pp. 9–51). Rome: Tipografia Poliglotta Vaticana.

Coarelli, F. (1988). *Il Foro Boario: dalle origini alla fine della Repubblica*. Rome: Quasar.

D'Ambrosio, E., Marra, F., Cavallo, A., Gaeta, M., & Ventura, G. (2015). Provenance materials for Vitruvius' *harenae fossiciae* and *pulvis puteolanis*: geochemical signature and historical-archaeological implications. *Journal of Archaeological Science: Reports*, **2**, 186–203.

Diffendale, D. P. (2016). On the supposed building program of M. Fulvius Flaccus. In P. Brocato, M. Ceci, & N. Terrenato (Eds.), *Ricerche nell'area dei templi di Fortuna e Mater Matuta. I* (pp. 141–166). Arcavacata di Rende: Università della Calabria.

Diffendale, D. P., Brocato, P., Terrenato, N., & Brock, A. L. (2016). Sant'Omobono: an interim *status quaestionis*. *Journal of Roman Archaeology*, **29**, 7–42.
doi:10.1017/S1047759400072032.

Farr, J., Marra, F., & Terrenato, N. (2015). Geochemical identification criteria for “peperino” stones employed in ancient Roman buildings: a Lapis Gabinus case study. *Journal of Archaeological Science: Reports*, **3**, 41–51.

Freda, C., Gaeta, M., Karner, D. B., Marra, F., Renne, P. R., Taddeucci, J., Scarlato, P., Christensen, J. N., & Dallai, L. (2006). Eruptive history and petrologic evolution of the Albano multiple maar (Alban Hills, Central Italy). *Bulletin of Volcanology*, **68**, 567–591.

Frank, T. (1924). *Roman Buildings of the Republic: An Attempt to Date Them from Their Materials*. Rome: American Academy in Rome.

Germinario, L., Hanchar, J. M., Sassi, R., Maritan, L., Cossio, R., Borghi, A., & Mazzoli, C. (2018a). New petrographic and geochemical tracers for recognizing the provenance quarry of trachyte of the Euganean Hills, northeastern Italy. *Geoarchaeology*, **33**, 430–452.

Germinario, L., Zara, A., Maritan, L., Bonetto, J., Hanchar, J. M., Sassi, R., Siegesmund, S., & Mazzoli, C. (2018b). Tracking trachyte on the Roman routes: Provenance study of Roman infrastructure and insights into ancient trades in northern Italy. *Geoarchaeology*, **33**, 417–429.

Holloway, R. R. (1994). *The archaeology of early Rome and Latium*. London-New York: Routledge.

Jackson, M. D., Marra, F., Hay, R. L., Cawood, C., & Winkler, E. M. (2005). The Judicious Selection and Preservation of Tuff and Travertine Building Stone in Ancient Rome. *Archaeometry*, **47**, 485–510.

Jackson, M. D., & Marra, F. (2006). Roman Stone Masonry: Volcanic Foundations of the Ancient City. *American Journal of Archaeology*, **110**, 403–436.

Karner, D. B., Lombardi, L., Marra, F., Fortini, P., & Renne, P. R. (2001). Age of Ancient Monuments by Means of Building Stone Provenance: a Case Study of the

Tullianum, Rome, Italy. *Journal of Archaeological Science*, **28**, 387–393. doi:10.1006/jasc.2000.0567

Lugli, G. (1957). *La tecnica edilizia romana con particolare riguardo a Roma e Lazio*. Rome: Bardi.

Lustrino, M., Duggen, S., & Rosenberg, C. L. (2011). The Central-Western Mediterranean: Anomalous igneous activity in an anomalous collisional tectonic setting. *Earth-Science Reviews*, **104**, 1–40.

Marchetti Longhi, G. (1932). Gli scavi di Largo Argentina. *Bullettino della Commissione Archeologica Comunale di Roma*, **60**, 253–346.

Marra, F., Deocampo, D., Jackson, M. D., & Ventura, G. (2011). The Alban Hills and Monti Sabatini volcanic products used in ancient Roman masonry (Italy): an integrated stratigraphic, archeological, environmental and geochemical approach. *Earth-Science Reviews*, **108**, 115–136. doi: 10.1016/j.earscirev.2011.06.005.

Marra, F., & D'Ambrosio, E. (2013). Trace-element classification diagrams of pyroclastic rocks from the volcanic districts of Central Italy: the case study of the ancient Roman ships of Pisa. *Archaeometry*, **55** (6), 993–1019. doi: 10.1111/j.1475-4754.2012.00725.x

Marra, F., D'Ambrosio, E., Gaeta, M., & Mattei, M. (2015). Petrochemical Identification and Insights on Chronological Employment of the Volcanic Aggregates Used in Ancient Roman Mortars. *Archaeometry*, **58** (2), 177–200. doi: 10.1111/arc.12154

Marra, F., D'Ambrosio, E., Gaeta, M., & Mattei, M. (2017). Geochemical fingerprint of Tufo Lionato blocks from the *Area Sacra di Largo Argentina*: implications for the chronology of volcanic building stones in ancient Rome. *Archaeometry*, DOI: 10.1111/arc.12343

Mercando, L. (1966). Saggi di scavo sulla platea dei templi gemelli. *Bullettino della Commissione Archeologica Comunale di Roma*, **79**, 34–67.

Peccerillo, A. (2005). *Plio-Quaternary volcanism in Italy: Petrology, geochemistry, geodynamics*. Berlin: Springer-Verlag.

Pisani Sartorio, G. (1970). Area dei Templi della Fortuna e Mater Matuta (Area Sacra di S. Omobono). Unpublished 1:50 scale site plan (S. Omobono, b. 33, 4039–4040), Archivio Sovrintendenza Roma Capitale – Monumenti, Rome, Italy.

Quilici, L. (1974). *Collatia*. Rome: De Luca.

Sommella, P. (1968). Area sacra di S. Omobono. Contributo per una datazione della platea dei templi gemelli. *Quaderni dell'Istituto di Topografia Antica della Università di Roma*, **5**, 63–70.

Terrenato, N., Brocato, P., Caruso, G., Ramieri, A. M., Becker, H. W., Cangemi, I., Mantiloni, G., & Regoli, C. (2012). The S. Omobono Sanctuary in Rome: Assessing eighty years of fieldwork and exploring perspectives for the future. *Internet Archaeology*, **31**, (http://intarch.ac.uk/journal/issue31/terrenato_index.html).

This article is protected by copyright. All rights reserved.

Torelli, M. (1968). Il donario di M. Fulvio Flacco nell'area di S. Omobono. *Quaderni dell'Istituto di Topografia Antica della Università di Roma*, 5, 71–76.

Figures

Figure 1. The archaeological site of Sant'Omobono.



Figure 2. Geological map of the vicinity of Rome, with insets showing known Anio, Monteverde, and Portuense quarry sites, along with the city center indicating locations of archaeological sites discussed in the text.

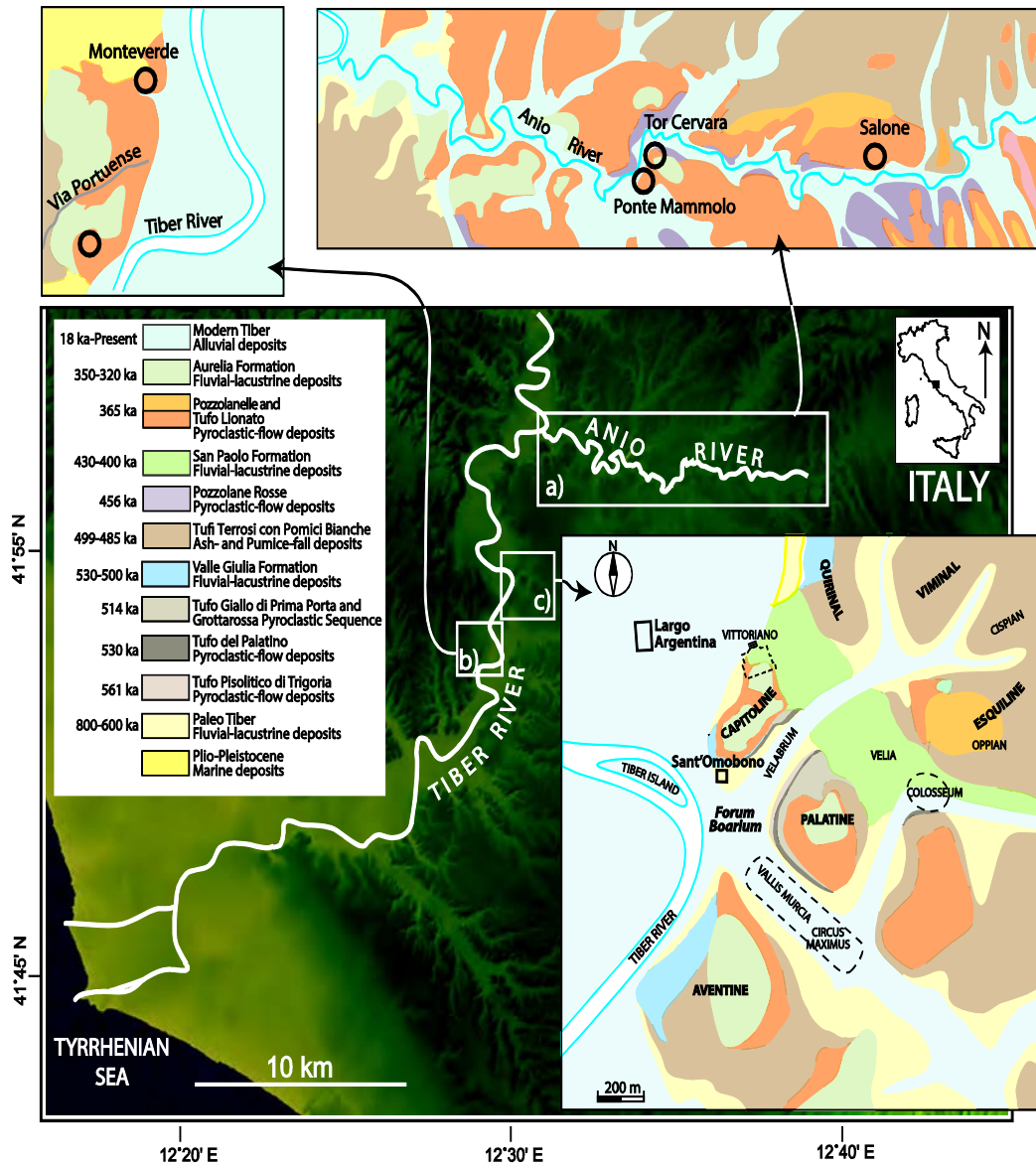


Figure 3. Plan of samples taken for geochemical analysis from the Temples of Fortuna and Mater Matuta at Sant'Omobono, Rome.

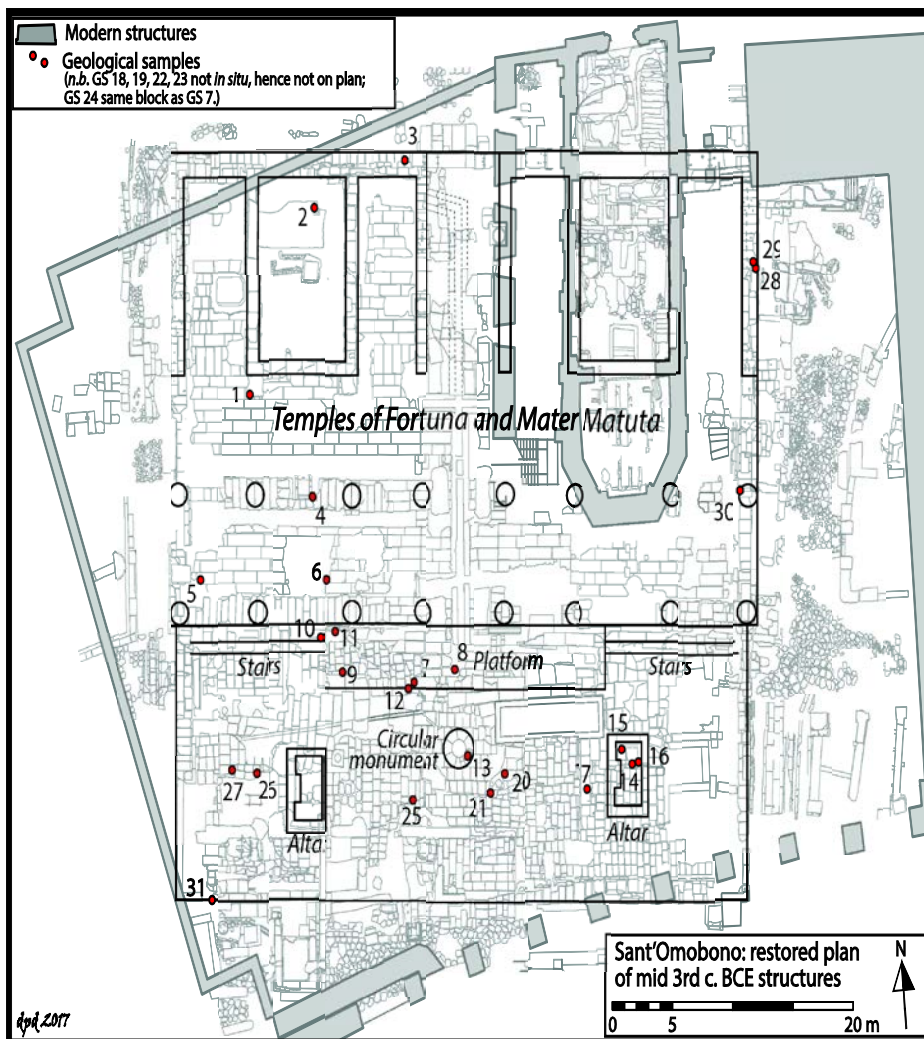


Figure 4. Photographs of tuff samples showing varying macroscopic aspect, from a rock facies (MV) similar to that of the Tufo Lionato cropping out in Monteverde (sample MV-A), to that typical of the Tufo Lionato cropping out in the Anio River valley (AN). Legend: L: Leucite crystal; G: Grey scoria; C: Carbonate lithic clast.

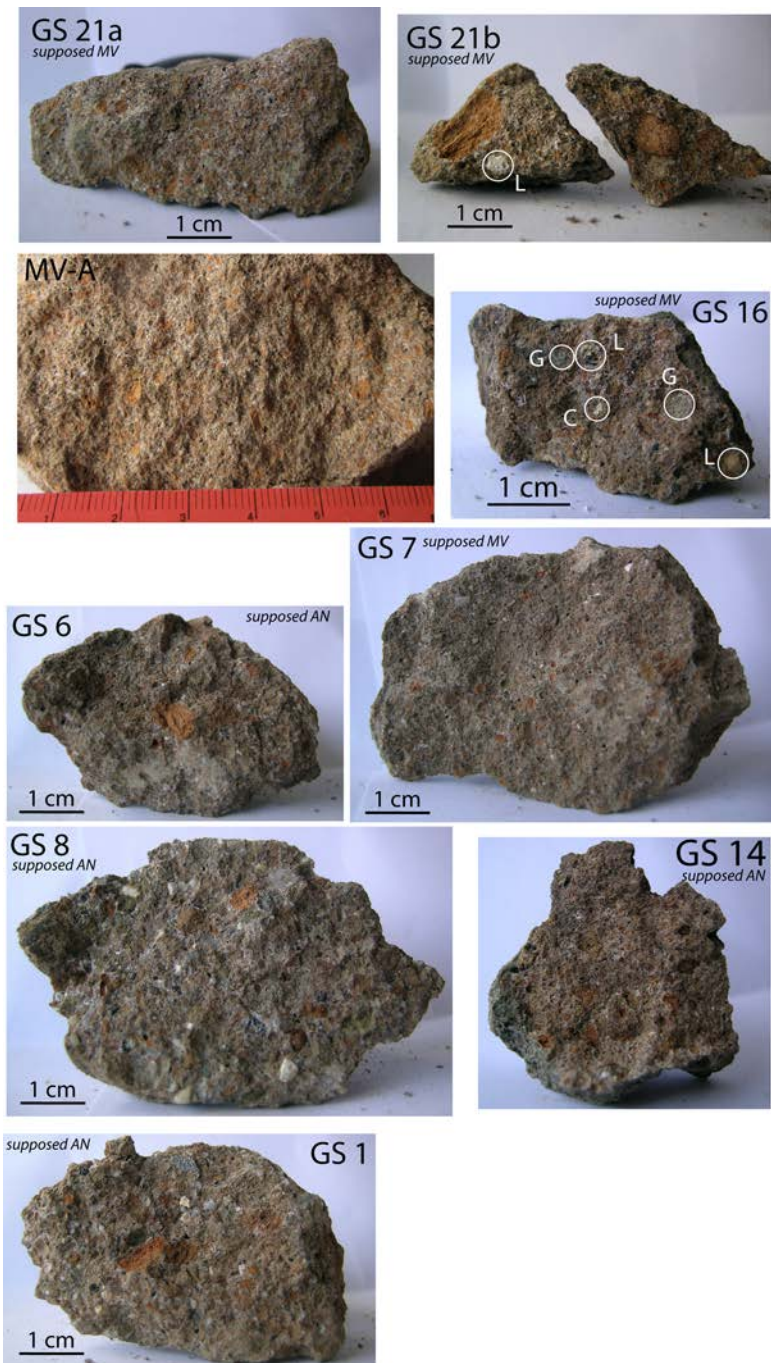


Figure 5. Photomicrographs showing textural features of Tufo Lionato (Anio facies, sample GS16). (a) Ghost of euhedral leucite characterized by a cloudy, white color due to the substitution of leucite with secondary minerals (plane-polarized light). (b) Detail of ghost leucite showing that the original crystal is turned into calcite at the core and into zeolite at the rim (cross-polarized light).

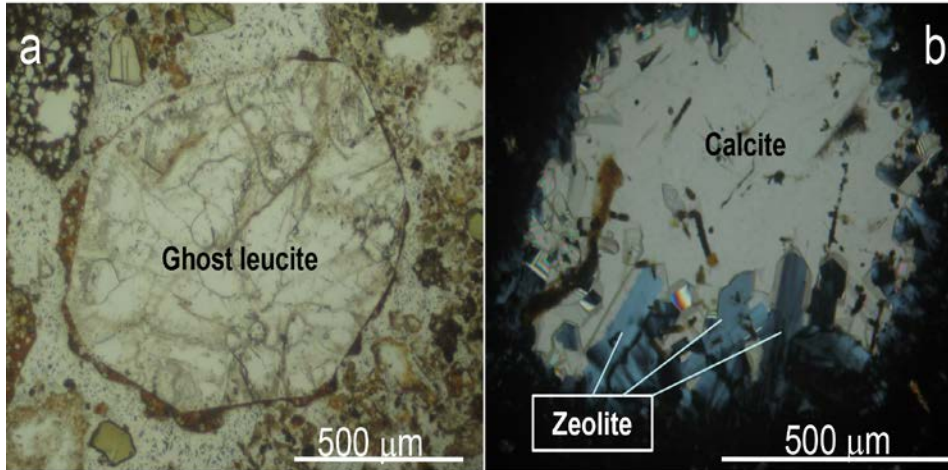


Figure 6. Zr/Y vs Nb/Y discrimination diagram showing composition of the analyzed tuff samples (open circles). Compositional fields for the different rock facies of Tufo Lionato defined based on outcrop samples (filled circles) analyzed in Marra et al. 2017, and for Tufo del Palatino, Lapis Gabinus, and Lapis Albanus previously defined in Farr et al. 2015, are shown for comparison. A solid red line separates the Anio (AN) and Monteverde (MV) compositional fields determined in Marra et al. 2017. The dashed red line indicates the AN-MV divide adjusted to take account of the composition of two control samples (X-1, X-2) from the Anio quarries.

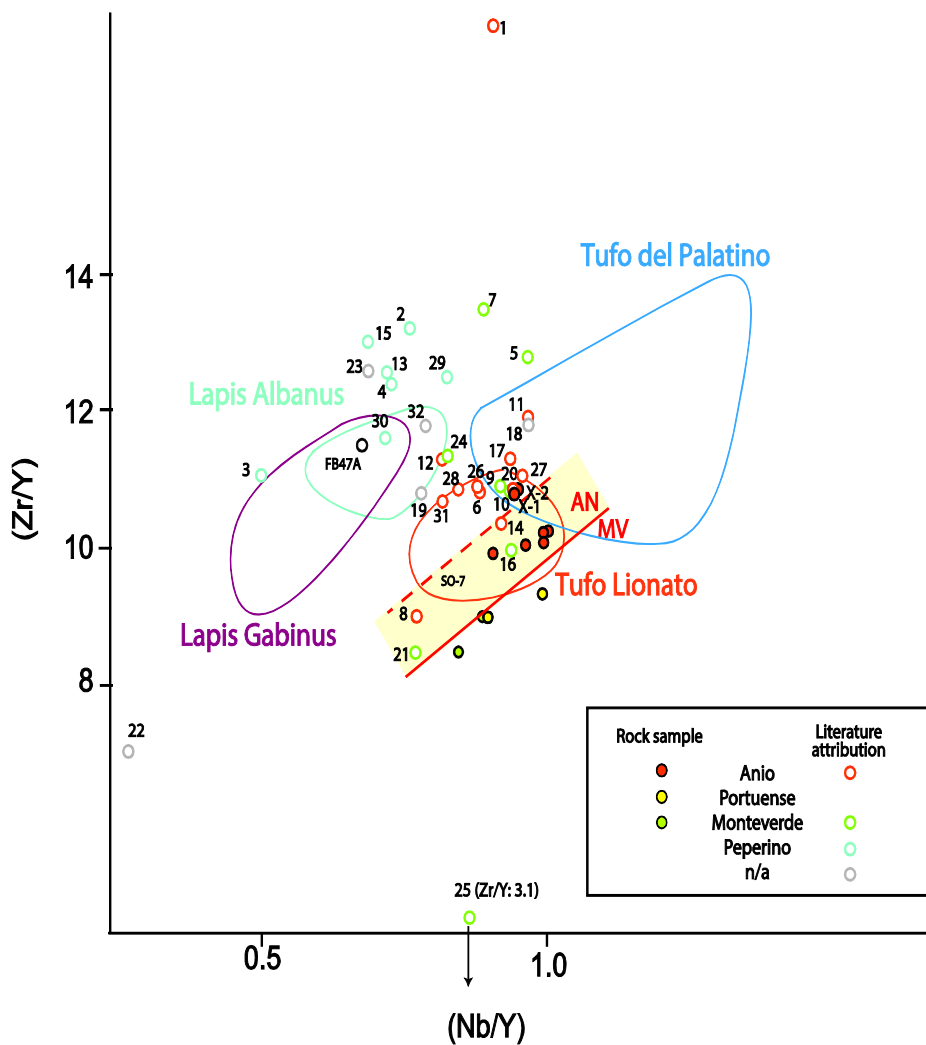


Figure 7. Th/Ta vs Nb/Zr discrimination diagram showing composition of the analyzed tuff samples (open circles). Compositional fields for the different rock facies of Tufo Lionato defined based on outcrop samples (filled circles) analyzed in Marra et al. (2017), and for Tufo del Palatino, Lapis Gabinus, and Lapis Albanus previously defined in Farr et al. (2015), are shown for comparison. A solid red line separates the Anio (AN) and Monteverde (MV) compositional fields determined in Marra et al. 2017. The dashed red line indicates the AN-MV divide adjusted to take account of the composition of two control samples (X-1, X-2) from the Anio quarries.

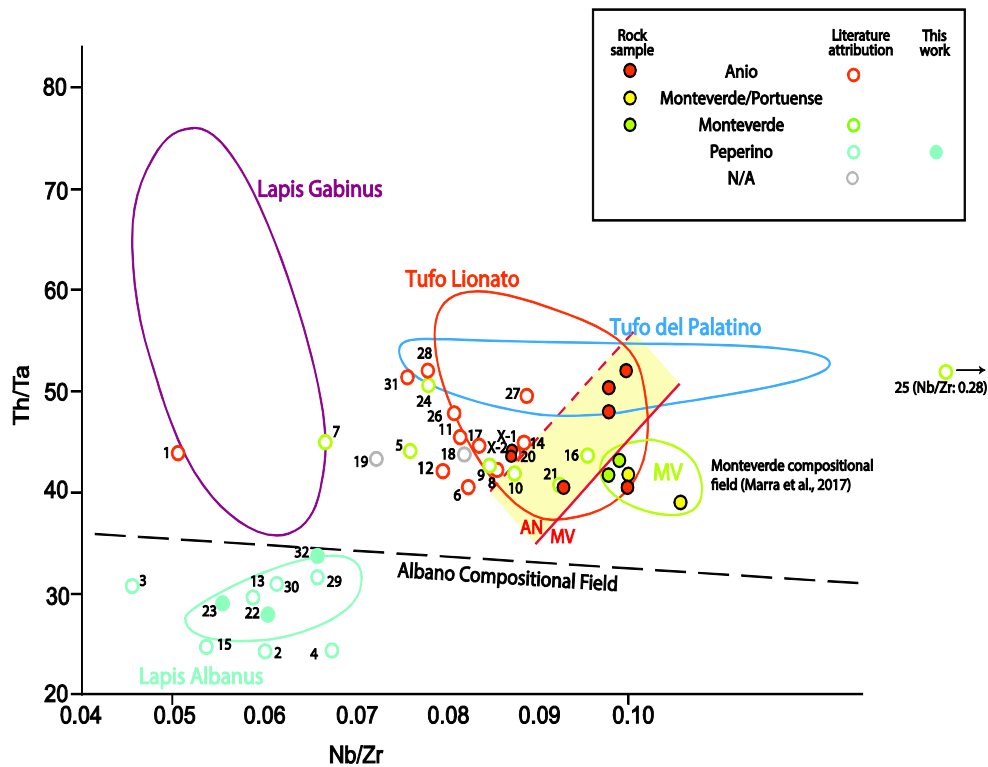


Figure 8. Th/Ta vs Nb/Y discrimination diagram showing composition of the analyzed tuff samples (open circles). Compositional fields for the different rock facies of Tufo Lionato defined based on outcrop samples (filled circles) analyzed in Marra et al. (2017), and for Tufo del Palatino, Lapis Gabinus, and Lapis Albanus previously analyzed in Farr et al. (2015), are shown for comparison.

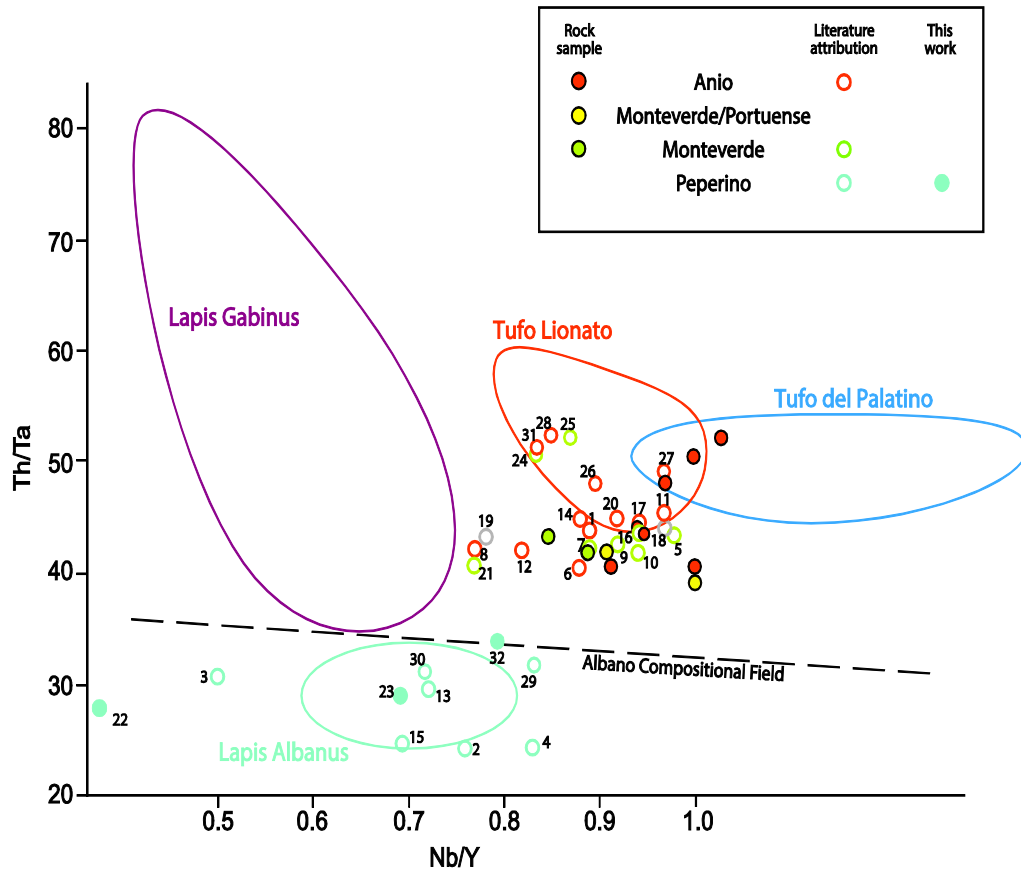


Table 1. List of Analyzed Tuff Samples

Sample	Geochemical attribution	Arch. structure¹	Archaeological date²	Previous attribution³
9	TL – Anio	Block pavement	4th or early 3rd c.	Monteverde
21	TL – Anio**	Block pavement	4th or early 3rd c.	Monteverde
25	TL – Anio	Block pavement	4th or early 3rd c.	Monteverde
26	TL – Anio	Block pavement	4th or early 3rd c.	Anio
27	TL – Anio	Block pavement	4th or early 3rd c.	Anio
14	TL – Anio*	Eastern altar foundation	4th or early 3rd c.	Anio
16	TL – Anio**	Eastern altar foundation	4th or early 3rd c.	Monteverde
17	TL – Anio	Eastern altar platea	4th or early 3rd c.	Anio
19	TL – Anio	Column base or capital	4th–3rd c.	N/A
1	TL – Anio	Slab pavement	Early 3rd c.	Anio
5	TL – Anio	Slab pavement	Early 3rd c.	Monteverde
6	TL – Anio	Slab pavement	Early 3rd c.	Anio
7	TL – Anio	Slab staircase	Early 3rd c.	Monteverde
24	TL – Anio	Block = GS 7	Early 3rd c.	Monteverde
8	TL – Anio*	Slab staircase	Early 3rd c.	Anio
10	TL – Anio	Slab staircase	Early 3rd c.	Monteverde
11	TL – Anio	Drain	Early 3rd c.?	Anio
12	TL – Anio	Slab staircase	Early 3rd c.	Anio
31	TL – Anio	Facing of podium	3rd c.	Anio
20	TL – Anio	Thin slab pavement	212	Anio
28	TL – Anio	Facing of podium	212	Anio
18	TL – Anio	Column drum	Late 3rd c. or later	N/A
30	Lapis Albanus	Facing of podium	5th c.	Peperino
3	Lapis Albanus	Facing of podium	5th c.	Peperino
13	Lapis Albanus	Circular monument base	4th or early 3rd c.?	Peperino
15	Lapis Albanus	Eastern altar molding	4th or early 3rd c.	Peperino
2	Lapis Albanus	Cippus/statue base	3rd c.	Peperino
22	Lapis Albanus	Fulv. Flaccus inscription	264	N/A
32	Lapis Albanus	Fulv. Flaccus inscription	264	N/A
29	Lapis Albanus	Facing of podium	212	Peperino
4	Lapis	Lining of votive pit	Late 3rd c. or later	Peperino

	Albanus			
23	Lapis Albanus	Stair tread	Medieval or later	N/A

** Supposed Monteverde facies displaying trace-element composition close to Monteverde.

* Supposed Anio facies displaying trace-element composition close to Monteverde.

Samples selected for thin section

¹ As defined in Diffendale et al., 2016. ² All dates BCE, other than for Sample 23. ³ According to Pisani Sartorio, 1970.

Table 2. Essential textural features of Tufo Lionato facies (Marra et al., 2017).

Lithotype	Texture	Grain size	Sorting	Matrix	Juvenile fraction	Glass features	Loose crystals	Lithic clasts
Anio facies	Matrix supported	Lapilli to fine ash	Poor	Abundant with calcite and zeolite	Glassy and vesiculated, from aphyric to highly porphyritic with clinopyroxene and mica phenocrysts	Orange to black in color, vesicles, sometimes elongated, are commonly filled by calcite and zeolite	Abundant leucite generally turned into calcite and zeolite, clinopyroxene (euhedral, from colorless to pleochroic: green to brown-gold) and mica; scarce garnet, oxide, and sanidine	Leucite- and clinopyroxene-bearing lava and scoria; rare garnet-bearing granular rocks and fine grained limestone,
Monteverde facies	Clast supported with clasts coated by a zeolite film	Coarse ash	Relatively good	Scarce and completely turned into zeolite	Glassy and vesiculated, generally aphyric	Orange in color, vesicles, sometimes elongated, are commonly filled by zeolite	Abundant clinopyroxene (euhedral, green to brown-gold) and mica (thin, elongated and roughly orientated); scarce leucite (generally turned into calcite and zeolite),	Scarce, fine grained limestone

							sanidine, garnet, and oxide.	
Portuense facies	Clast supported	Fine ash with scarce coarse ash	Relative ly good	Glassy with scarce zeolite	Glassy and vesiculated, generally aphyric	Orange to red in color with vesicles, sometimes s elongated, filled by zeolite	Orientated, submillimeter to millimeter mica; scarce leucite (completely turned into zeolite) clinopyroxene , sanidine, and oxide	Not occurring at thin section scale